Digest Journal of Nanomaterials and Biostructures Vol. 11, No. 4, October-December 2016, p. 1361-1366

NUMERICAL SIMULATION OF MULTI-QUANTUM WELL SOLAR CELLS GaAs / InAs USING SILVACO ATLAS

A. TALHI[a,b*], A. BELGHACHI[b], H. MOUGHLI[b], B. AMIRI[b], L. VARANI[c]
[a]*University Centre of Tindouf, Algeria*
[b]*Laboratory of semiconductor devices physics, University of Bechar, Algeria*
[c]*Institut d'Electronique et des Systèmes, University Montpellier 2, France*

Inserting Multi-quantum well into solar cells proved to be a promising technique for producing high efficiency third generation solar cells. The presence of quantum well increases the absorption spectra into longer wavelengths, therefore increasing the short-circuit current density while maintaining the open-circuit voltage at acceptable level. The calculation of threshold wavelength necessitates numerical resolution of Schrödinger equation in order to obtain the effective forbidden band-gap for every Multi-Quantum Well Solar Cells (MQWSC) configuration; well thickness, barrier width and number of wells. In this work; MQWSC InAs/GaAs solar cell is simulated using a numerical semiconductors devices simulator (SILVACO TCAD). Calculation of the effective forbidden band-gap is carried out using a Matlab program. The investigated technological parameters are: number of wells, thickness of well and barrier. Our simulation shows that increasing number of wells in the intrinsic region of GaAs/InAs/GaAs structure increases efficiency for narrow wells (< 8 nm) while it decreases for wider wells (> 9nm). An optimised cell is obtained where an efficiency exceeding 27% can be obtained; this value is clearly greater than the zero quantum well structure 22%.

(Received October 4, 2016; Accepted December 16, 2016)

Keywords: Multi-quantum well; solar cell, SILVACO, Schrödinger equation.

1. Introduction

The quantum well solar cell (QWSC) was first introduced by Barnham and co-workers [1] as a novel device in which a series of quantum wells (QWs) forms the *i*-layer of a *p*-*i*-*n* solar cell. Studies have shown that the insertion of such a series of quantum wells into the depletion region of a solar cell can significantly enhance the cell's short-circuit current and hence the efficiency of the solar cell [2, 3]. Higher photocurrent can be generated if wells are deeper, since longer wavelengths are then absorbed [4]. The incorporation of the multiple quantum wells (MQWs) has two counteracting effects: the short-circuit current is increased because of the additional absorption of low-energy photons in the lower band-gap quantum wells; and the open-circuit voltage is decreased because of the increased recombination of carriers trapped in the quantum wells [5]. The photocurrent is then determined by lower-band-gap (well) material, while the output voltage would be determined by barrier material. The characteristics of the well, its width and depth, determine the absorption edge and the spectral response of the MQW solar cell. Longer wavelengths can be absorbed if the quantum well is deeper, leading to a higher photocurrent in the cell. Whereas, the output voltage is related to the width of the host material band gap, the recombination in the well and interfaces between barriers and wells. Therefore, in choosing the depth of the wells one has to compromise between the photocurrent and the output voltage. The number of wells is an important factor too, wider wells improve the absorption, but a smaller number of wells fit in the intrinsic region. Whereas, a large number of narrow wells with lower

*Corresponding author: karim.talhi@gmail.com

photon absorption can be inserted in the same intrinsic layer. Increasing the number of wells enhances the photocurrent provided the recombination at the interfaces is reduced.

2. Device description

The solar cell studied here are p-i-n structure where the i-region consist of MQW ranging from 1 to 15 wells, this structure is obtained with alternating GaAs and InAs (Fig 1).The top layer n-type GaAs emitter is doped at 2×10^{18} cm^{-3} and the bottom p-type GaAs base is doped at 1×10^{18} cm^{-3}, 0.5 µm and 10 µm were applied respectively. In the intrinsic region, 1 µm; there are GaAs barriers and InAs quantum wells. Silvaco TCAD electronic devices numerical simulator is used to simulate this solar cell under standard conditions and AM1.5 spectrum. Detailed of material parameters shown in table 1used in our simulation.

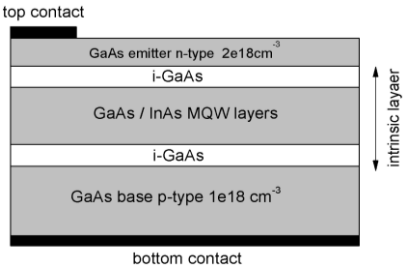

Fig.1. Schematic drawing of MQW cells

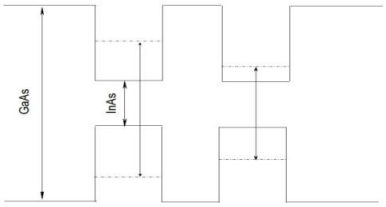

Fig 2 Schematic band diagram p GaAs-InAs(MQW)-n GaAs Solar Cell (GaAs=1.42 eV;InAs=0.32 eV)

Table 1 Major parameter used in simulation [8]

Layers Parameters	Emitter layer n-type GaAs	Base layer p-type GaAs	Intrinsic layer	QW InAs
Thickness (µm)	0.5	10	01	5 nm to 10 nm
Dielectric constant, ε	13.1	13.1	/	15
Electron mobility μ_n(cm^2/Vs)	8800	8800	/	30000
Hole mobility μ_p(cm^2/Vs)	400	400	/	240
Carrier density, *n* or *p* (cm^{-3})	2×10^{18}	1×10^{18}	/	/
Optical band gap, *Eg*(eV)	1.42	1.42	/	0.36
Effective density, *Nc*(cm^{-3})	4.7×10^{17}	4.7×10^{17}	/	8.7×10^{16}
Effective density, *Nv*(cm^{-3})	7×10^{18}	7×10^{18}	/	6.6×10^{18}

4. Modelling software Silvaco Atlas

In this paper we used the Silvaco atlas for modelling of quantum well solar cell to calculate the different parameters of this solar cell. Silvaco Atlas was used to execute the code in which we had modelled the multi quantum well solar cell and input the parameters accordingly so as to maximize the output efficiency [6]. The curves of simulations were viewed in Tonyplot and output log files were produced.

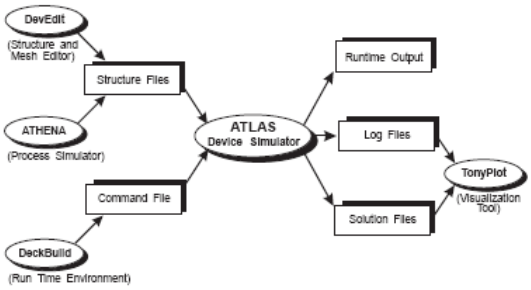

Fig 3 Atlas Silvaco inputs and outputs [7]

There are some steps must be followed when writing a Silvaco Atlas code .Figure 4 gives what these steps are[6]. In Silvaco Tcad, first of all the structure must made up by defining the boundaries and the points in the structure .Secondly the electrode and concentration doping are defined. After structure, the material parameters; physical models are defined. Numerical method selection is choosing to calculate the model of simulation. Finally the solutions saved in LOG files and plot the curves in TONYPLOT.

Group	*Statements*
1. Structure Specification	MESH REGION ELECTRODE DOPING
2. Material Models Specification	MATERIAL MODELS CONTACT INTERFACE
3. Numerical Method Selection	METHOD
4. Solution Specification	LOG SOLVE LOAD SAVE
5. Results Analysis	EXTRACT TONYPLOT

Fig 4: Atlas Command Groups with the Primary Statements in each Group [7]

5. Results and discussion

5.1. Effective Energy band-gap Levels:

In Fig.5 is shown the effective energy band-gap versus the width of well for different barrier thicknesses. By definition, the effective energy band-gap is the difference between the highest bound energy level in the valence band and the lowest bound energy level of the conduction band. These bound energies are obtained by a numerical simulation of Schrödinger equation for one quantum well. One notices a rating decrease of the effective energy band-gap value when increasing the width of the well together with an overall decrease when the barrier becomes thicker. We can see that the effective E_g can be tailored, thus allowing a considerable shift of the threshold of absorption from *0.645 eV* for ultra-thin InAs wells to *0.44 eV* thick films. For photovoltaic application low energy band-gap allows high absorption probability while this

leads to low open-circuit voltage. To extract the maximum power from a cell the two competing mechanisms one has to find the optimal point with the optimal band-gap.

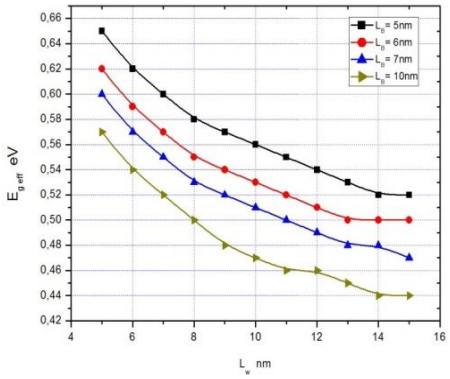

Fig 5 Effective energy vs. well width at constant barrier width

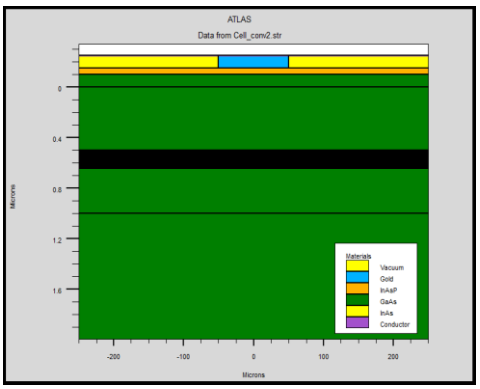

Fig 6 Structure of MQWSC in Silvaco Atlas

5.2. Well Thickness and Number Optimization:

Fig.7 is the efficiency of the solar cell according to the number of wells and the well width for a constant barrier thickness L_B = 10 nm. We can distinguish two different behaviours; the first, for low well widths ($L_w \leq 7$ nm), where a significant increase of efficiency is obtained when the number of wells is increased. The second behaviour is observed for higher well widths ($L_w \geq 8$ nm), in this range the efficiency drops steadily if the number wells is increased. The effect of the barrier thickness has little effect on this result, several calculations were carried out for different barrier thicknesses and negligible effect is reported, provided that this thickness is greater than the well width to insure uncoupled wells condition. The case thin barrier thickness is also examined, fig. 8 shows the case of L_B = 5 nm and for L_w= 5nm, 10nm and 15 nm, the same previous behaviour is obtained, confirming that the barrier thickness has little effect. In Fig.7 the case of no-quantum well is also plotted for comparison, the simulated GaAs p-i-n solar cell yield an efficiency of *22%*, this value is clearly lower than that of MQW case for $L_w \leq 7$ *nm*, particularly if the number of wells exceeds *6 QWs*. The enhanced efficiency for low quantum well width could be attributed not only to the improved absorption because of the low band-gap but also to relatively larger effective band gap associated with ultra-thin wells, this can be seen in figure 8. Ultra-thin InAs wells produces relatively larger band-gaps (Fig.5) around *0.6eV* which is higher than bulk InAs band-gap of *0.354 eV*, therefore this will increase the photocurrent by the absorption of lower energy photons. This will also be less affecting the open-circuit voltage.

The number of wells in a structure is determined by the thickness of the intrinsic layer. When increasing the number of wells the rate of lower band-gap (effective band-gap) to larger band-gap (GaAs band-gap) is increased. For high effective band-gaps (close to the barrier band-gap) the efficiency increases with the number of wells. Whereas, for very low effective band-gaps (close to bulk InAs band-gap), increasing the number of wells degrades remarkably the efficiency.

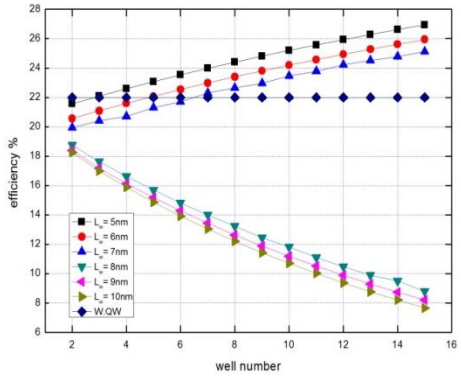

Fig 7 Efficiency vs. well number at Constant barrier L_B=10 nm

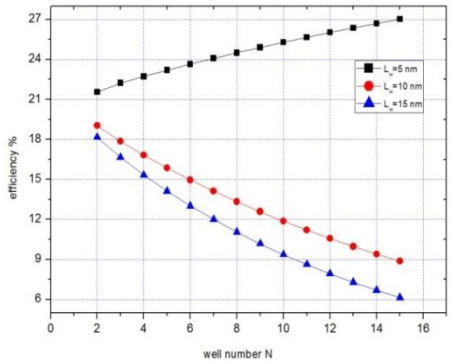

Fig 8 Efficiency vs. well number at constant barrier width L_B= 5 nm

6. Conclusions

The simulation of MQWSC base on GaAs/InAs/GaAs compounds proves that a maximum efficiency of 27% can be reached. This efficiency is clearly above the simulated simple GaAs solar cell which is 22%. In the simulated structure the intrinsic layer is only 1µm and the maximum number of wells treated is 15. If these two parameters are further increased the performance of this structure could be improved. On the other hand the lower well width examined is 5 nm, with the development of new deposition techniques where the ultra-thin films can be produced the efficiency could be boosted not only because of high effective band-gap but also because of the number of wells that could be further increased in the same intrinsic layer. We have shown also that Silvaco ATLAS device simulator is able to simulate basic solar cell performance.

References

[1] K.W.J. Barnham and G. Duggan, A new approach to high-efficiency multi-band-gap solar cells, J. Appl. Phys. **67** (1990) 3490.

[2] J.C. Rimada, L. Hernandez, J.P. Connolly, K.W.J. Barnham, Conversion efficiency enhancement of AlGaAs quantum well solar cells, Microelectronics Journal **38** (2007) 513.

[3] X.B. Xiang, W.H. Du, X.L. Chang, H.R. Yuan, The study on high efficient Al*x*Ga*1-x*As/GaAs solar cell, Solar Energy Materials & Solar Cells **68** (2001) 97.
[4] Joanna Prazmowska, Ryszard Korbutowicz , Optimization of multi quantum well solar cell, Optica Applicata ,Vol XXXV, N°3,2005.
[5] Stephen M. Ramey and Rahim Khoie, Modeling of Multiple-Quantum-Well Solar Cells Including Capture, Escape, and Recombination of Photoexcited Carriers in Quantum Wells, IEEE transactions on electron devices, vol. 50, no. 5, may 2003 p 1179.
[6] Priyanjan.Sharma, Nitesh Malhotra, Ayush Tyagi, Akshay Pareek ,Anu Mehra, Preeti Singh and R.M.Mehra;Modeling of InGaN solar cell for better usage using Silvaco Atlas;ARPN journal of engineering and applied sciences;Vol10;N°10 august 2015
[7] Atlas User's Manual Device Simulation Software **;** Silvaco, Inc. 4701 Patrick Henry Drive, Bldg. 2 Santa Clara, CA 95054 October 2, 2013.
[8] Sadao Adachi**,** Properties of Semiconductor Alloys: Group-IV, III–V and II–VI Semiconductors, 2009 John Wiley & Sons, Ltd ISBN: 978-0-470-74369-0